Hindawi
Mathematical Problems in Engineering
Volume 2018, Article ID 8540546, 7 pages
https://doi.org/10.1155/2018/8540546

*Research Article*

# Dynamic Analysis of Slider-Crank Mechanism with a Cracked Rod

**Shouguo Cheng[1,2] and Shulin Liu[1]**

[1]*School of Mechatronics Engineering and Automation, Shanghai University, Shanghai, China*
[2]*Department of Mechanical and Electrical Engineering, Jiangyin Polytechnic College, Jiangyin, China*

Correspondence should be addressed to Shulin Liu; lsl346@126.com

Received 30 April 2018; Revised 1 August 2018; Accepted 15 August 2018; Published 2 September 2018

Academic Editor: Ricardo Perera



The dynamical equation of the slider-crank mechanism is established by using Lagrange equation and Newton's second law. The slider-crank mechanism with an open crack rod is investigated and then establishes the equivalent mechanics model by a massless torsional spring to simulate the influence of the crack in the rod, and the mechanism of a cracked rod is divided into two subsystems. The dynamical equation of the slider-crank mechanism with a crack rod is established. Comparing the dynamic analysis results between with and without crack in the rod, the results show that the existence of the crack leads to a great change in the motion characteristics of the slider. The calculated maximum Lyapunov exponent is positive, which shows that the movement of the slider in the crank slider mechanism with a cracked rod is chaotic.

## 1. Introduction

The precise relationship between the input and output is important for slider-crank mechanism [1]. For example in certain application, the rotation of crank is considered as the input and the displacement of the slider is considered as the output. Since the mechanism is not manufactured perfectly and cracks always exit which is known to be the source to reduce system reliability and precision [2, 3]. Moreover, it is difficult to calculate the influence by normal formula directly, if there is a crack in the rod. This kind of crack in the rod may cause the mechanism to exhibit nonlinear behaviour which should influence the mechanism dynamic when rod is activated according to crank rotating. So, this behaviour should be studied. Jin Zeng, HuiMa, Wensheng Zhang and RangchunWen mix elements by combining beam elements and solid elements to establish the finite element (FE) model for cracked cantilever beams and use the area damage factor to evaluate the crack levels [4]. Ugo Andresus, Paolo Casini use 2D quadrilateral to model the beam, then the natural frequencies (and the associated mode shapes) of the cracked cantilever beam were obtained [5], and they also use two-dimensional finite elements to consider the cantilever beam with an asymmetric edge crack as the plan problem and then conclude the behaviour of breathing crack which is simulated as a frictionless contact problem [6, 7]. Mihai Dupac and David G.Beale model the crack in rob by massless torsional spring, but the slider-crank mechanism is modeled by one equation of motion [8]. Andrea Carpinteri, AndreaSpagnoli, and SabrinaVantadori build up a general linear hardening rule for the fibers and a linear-elastic law for the matrix to assume an elastic-plastic crack bridging model [9]. O.Giannini, P.Casini, and F.Vestroni use finite element that has a bilinear element matrix with the discontinuity passing through the origin to model the cracked zone of the beam [10]. Pier Francesco Cacciola and Giuseppe Muscolino model the cracked beam by finite elements in which the closing crack model is used to describe the damaged element [11]. Ugo Andreaus, Paolo Baragatti, Paolo Casini, and Daniela Iacoviello present wavelet analysis for crack detection and quantification in beams based on static method, then the spatial wavelet transform is proven to be effective after comparing with the experimental study [12].Maryna V. Menshykova, Oleksandr V. Menshykov, and Igor A. Guz use the boundary integral equation method to solve the fracture mechanics problem, and they impose the constraints to the normal and tangential components of the contact force and

the displacement discontinuity vectors to take the contact interaction of the crack faces into account[13].

In this work, a new idea is created to divide the slider-crank mechanism into two subsystems by crack point, and the crack is modeled by massless torsional spring. Cracked rod is modeled as two successive equal rods connected with massless torsional spring. In this method, it is much easier to simulate the system with multiple cracks and easier to program by C language. Comparing with the analysis results between the slider-crank mechanism with crack and without crack, the conclusion shows that it is necessary to study crack influence when analyzing the mechanical system dynamic performance and vibration characteristic.

## 2. Motion Analysis of a Slider-Crank Mechanism

In order to study the difference of slider-crank mechanism dynamic motion with and without crack in the rod, the equation will be created and simulation will be done based on the calculation.

*2.1. Equation of Motion on a Slider-Crank Mechanism without Crack in the Rod.* A slider-crank mechanism without crack in the rod is modeled in Figure 1 to study the effect of dynamic motion. A cyclic bending moment M is considered to crank the mechanism, and the rods OA and AB are considered to be rigid. The mechanism motion can be written as Lagrange equation and Newton's second law [14–17].

For this one degree of freedom mechanism, a designated value $\varphi$ is set as variable in the system, and M is the external moment. The crank angle $\varphi$ is the angle between rod OA and the horizontal direction. The length of the rod OA is $l_1$, and then the length of the rod AB is $l_2$. The mass of rod OA is $m_1$, and the mass of rod AB is $m_2$. Rod OA inertial mass is $J_1 = (m_1/l_1)\int_0^{l_1} x^2 d_x = (1/3)m_1 l_1^2$. Rod AB inertial mass is $J_2 = (m_2/l_2)\int_0^{l_2} x^2 d_x = (1/3)m_2 l_2^2$.The center velocity of rod AB is $v_{c0}$, and its center angular velocity is $\omega_{c0}$. $v_B$ represents the velocity of slider B. The total kinetic energy is $T = \sum_{n=1}^{3} T_n$, where $T_1$ is kinetic energy of rod OA, $T_2$ is kinetic energy of rod AB, and $T_3$ is kinetic energy of slider B. One can calculate the slider-crank mechanism kinetic energy by

$$T = \sum_{n=1}^{3} T_n = \frac{1}{2}J_1\dot{\varphi}^2 + \left(\frac{1}{2}m_2 v_{c0}^2 + \frac{1}{2}J_2\omega_{c0}^2\right) + \frac{1}{2}m_3 v_B^2 \quad (1)$$

The generalized force can be written as

$$\begin{aligned} Q_\delta &= \sum \frac{W_\delta}{\delta_\varphi} \\ &= \frac{\left(M\cdot\delta_\varphi + m_1 g\cdot l_1\cdot\cos\varphi\cdot\delta_\varphi + m_2 g\cdot l_1\cdot\sin\varphi\cdot\cos\varphi\cdot\delta_\varphi\right)}{\delta_\varphi} \quad (2) \\ &= M + m_1 g\cdot l_1\cdot\cos\varphi + m_2 g\cdot l_1\cdot\sin\varphi\cdot\cos\varphi \end{aligned}$$

One can write the Lagrange differential equation of motion for the slider-crank mechanism without crack as follows [18–21]:

$$\frac{d}{dt}\left(\frac{\partial T}{\partial\dot{\varphi}}\right) - \frac{\partial T}{\partial\varphi} = Q_\varphi \quad (3)$$

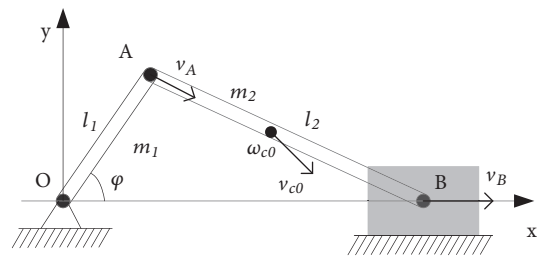


Figure 1: Slider-crank mechanism without crack in the rod.

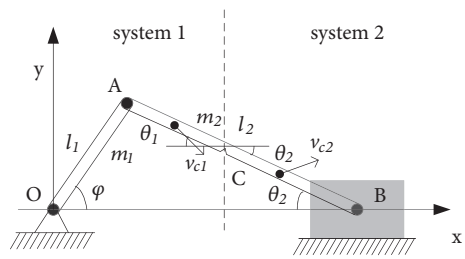


Figure 2: Slider-crank mechanism with a crack in the rod.

The solution for the function is given as follows:

$$\begin{aligned} &\frac{1}{3}m_1 l_1^2\ddot{\varphi} + m_2 l_1^2\ddot{\varphi} + \frac{13}{12}\frac{m_2 l_1^4\ddot{\varphi}}{l_2^2} + \frac{m_3 l_2^2\left(l_1^2 + l_2^2\right)\ddot{\varphi}}{l_2^2} \\ &\quad = M + m_1 g\cdot l_1\cdot\cos\varphi + m_2 g\cdot l_1\cdot\sin\varphi\cdot\cos\varphi \end{aligned} \quad (4)$$

*2.2. Equation of Motion on a Slider-Crank Mechanism with a Crack in the Rod.* A slider-crank mechanism with a crack in the rod is modeled in Figure 2 to study the effect of dynamic motion. Rod AB is considered to be composed of two rods AC and CB. Crack point C is at the middle of rod AB. A cyclic bending moment M is considered to crank the mechanism.

*2.2.1. System 1 and System 2 Dynamic Equations.* The slider-crank mechanism is considered as system 1 and system 2 which are divided by the crack. The equivalent mechanics model of the crack can be established by a massless torsional spring [22, 23].

For system 1, there are two degrees of freedom; two designated values $\varphi$ and $\theta_1$ are set as variable in the system. The crank angle $\varphi$ is the angle between rod OA and the horizontal direction. $\theta_1$is the angle between rod AC and the horizontal direction. The center velocity of rod AC is $v_{c1}$, and its center angular velocity is $\omega_{c1}$. The mass of rod AO is $m_1$, and the mass of rod AB is $m_2$. Because rod AO and rod AB are considered as material uniform distribution, the mass of rod AC $m_{c1}$ is $(1/2)m_2$. The total kinetic energy for system 1 is $T = \sum_{n=1}^{2} T_n$, where $T_1$ is kinetic energy of rod OA, $T_2$ is kinetic energy of rod AC. One can calculate the system 1 kinetic energy by the following formula:

$$T = \sum_{n=1}^{2} T_n = \frac{1}{2}J_1\dot{\varphi}^2 + \left(\frac{1}{2}m_{c1}v_{c1}^2 + \frac{1}{2}J_{c1}\omega_{c1}^2\right) \quad (5)$$

The generalized force can be written as

$$Q_\varphi = \sum \frac{W_\varphi}{\delta_\varphi} = \frac{M\delta_\varphi + m_1 g \cdot \cos\varphi \cdot (1/2)\,\delta_\varphi \cdot l_1 + (1/2)\,m_2 g \cdot \left(\delta_\varphi \cdot l_1 + (1/4)\,\omega_{c1} \cdot l_2\right) \cdot \cos\theta_1 + T_{c1} \cdot \omega_{c01}}{\delta_\varphi}$$
$$Q_{\theta 1} = \sum \frac{W_{\theta 1}}{\delta_{\theta 1}} = \frac{\left(T_{co1}\delta_{\theta 1} + (1/2)\,m_2 g \cdot \cos\theta_1 \cdot (1/4)\,\delta_{\theta 1} \cdot l_2 + M \cdot \delta_\varphi + m_1 g \cdot \cos\varphi \cdot (1/2) \cdot \delta_\varphi \cdot l_1\right)}{\delta_{\theta 1}} 0 \tag{6}$$

One can write the Lagrange differential equation of motion as follows [24]:

$$\frac{d}{dt}\left(\frac{\partial T}{\partial \dot\varphi}\right) - \frac{\partial T}{\partial \varphi} = Q_\varphi \quad (\dot\varphi = \delta\varphi)$$
$$\frac{d}{dt}\left(\frac{\partial T}{\partial \dot\theta_1}\right) - \frac{\partial T}{\partial \theta_1} = Q_{\theta_1} \tag{7}$$

The solution for the function is given as follows:

$$\begin{aligned}
&\frac{1}{3}m_1 l_1^2 \ddot\varphi + \frac{1}{2}m_2 l_1^2 \ddot\varphi + \frac{1}{8}m_2 \ddot\theta_1 l_1 l_2 \\
&\quad = M + \frac{1}{2}m_1 g \cdot \cos\varphi \cdot l_1 + \frac{1}{2}m_2 g \\
&\qquad \cdot \cos\theta_1 \cdot l_1 + \left(\frac{1}{8}m_2 g \cdot l_2 \cdot \cos\theta_1 + T_{c01}\right) \cdot \frac{\dot\theta_1}{\dot\varphi} \\
&\frac{1}{32}m_2 \ddot\theta_1 l_2^2 + \frac{1}{8}m_2 \ddot\varphi l_1 l_2 + \frac{1}{24}m_2 l_2^2 \theta_1 \\
&\quad = T_{c01} + \frac{1}{8}m_2 g \cos\theta_1 l_2 + \left(M + m_1 g \cdot \cos\varphi \cdot \frac{1}{2}l_1\right) \\
&\qquad \cdot \frac{\dot\varphi}{\delta_{\theta_1}}
\end{aligned} \tag{8}$$

For system 2, same as system 1, the generalized force can be written as

$$\begin{aligned}
Q_{\theta 2} &= \sum \frac{W_{\theta 2}}{\delta_{\theta 2}} \\
&= \frac{\left(T_{c02} \cdot \delta_{\theta 2} + (1/2) \cdot m_2 g \cdot \cos\theta_2 \cdot (1/4) \cdot l_2\right)}{\delta_{\theta 2}} \\
Q_S &= \sum \frac{W_s}{\delta_s} = F \cdot \frac{\delta_s}{\delta_s} = F
\end{aligned} \tag{9}$$

One can write Lagrange differential equation as follows:

$$\frac{d}{dt}\left(\frac{\partial T}{\partial \dot\theta_2}\right) - \frac{\partial T}{\partial \theta_2} = Q_{\theta_2}$$
$$\frac{d}{dt}\left(\frac{\partial T}{\partial \dot s}\right) - \frac{\partial T}{\partial s} = Q_s \tag{10}$$

The solution for the function is given as follows:

$$\frac{7}{24} \cdot m_2 \cdot l_2^2 \cdot \ddot\theta_2 = T_{c02} + \frac{1}{8} \cdot \frac{m_2 g \cdot \cos\theta_2 \cdot l_2}{\delta\theta_2}$$
$$m_3 \cdot \ddot s = F \tag{11}$$

The mass of rod CB is $(1/2)m_2$, and $m_3$ is the mass of slider B. $T_{co2}$ is the kinetic energy of rod CB. $\theta_2$ is the angle between rod CB and the horizontal direction. S is the distance for slider B. The center velocity of rod CB is $v_{c2}$, and its center angular velocity is $\omega_{c2}$. F is the external force on slider B.

*2.2.2. Cracked Rod Calculation.* The rod AB is considered as flexible, then, to simulate the crack by massless torsional spring [25–31], which is shown in Figure 3. Figure 3(a) is on crack dimension in the rod, and Figure 3(b) is on torsional spring.

The equation of the deflection curve is

$$\frac{d^4 y}{dx^4} + k^2 \cdot \frac{d^2 y}{dx^2} = 0 \tag{12}$$

where $k^2 = p/EI$, p is the generalized force, and EI is the bending stiffness.

The solution of (12) is

$$y(x) = D_1 + D_2 x + D_3 \sin(kx) + D_4 \cos(kx) \tag{13}$$

where y(x) is the deflection, and the cross section bending angle is $\theta(x)$, bending moment is M(x), and one can calculate shearing force as follows [32]:

$$\theta(x) = \frac{dy}{dx}$$
$$M(x) = -EI \cdot \frac{d^2 y}{dx^2} \tag{14}$$
$$Q(x) = \frac{dM}{dx} - P \cdot \frac{dy}{dx}$$

The flexible rod is considered as consistent on deflection, bending moment, and shearing force, so the relative angle of the torsional spring $\theta_c$ can be written as

$$\theta_c = \theta_1(x_c) - \theta_2(x_2) = \frac{C}{EI} M_1(x_c) \tag{15}$$

where $\theta_1(x_c)$ is the relative angle between upper rod and the crack position, and $\theta_2(x_c)$ is the relative angle between

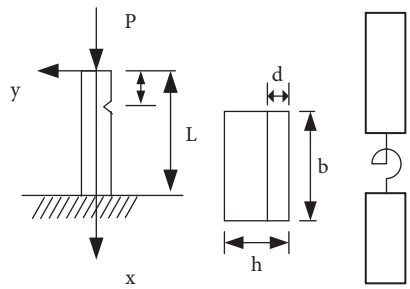


(a) Crack dimension in the rod (b) Torsional spring

Figure 3: The geometry of cracked rod.

lower rod and the crack position. The bending moment of the torsional spring is

$$M_1(x_c) = \frac{EI}{C} \cdot \theta_c \tag{16}$$

$$C = 5.346h\left(1.8624\varepsilon^2 - 3.95\varepsilon^3 + 16.375\varepsilon^4 - 37.226\varepsilon^5 + 76.81\varepsilon^6 - 126.9\varepsilon^7 + 172\varepsilon^8 - 143.97\varepsilon^9 + 66.56\varepsilon^{10}\right) \tag{17}$$

where C is the flexibility of the rotation spring which can be influenced by crack depth d and cross section height h [30, 33, 34].

$$\varepsilon = \frac{d}{h} \tag{18}$$

Then, the equation of slider-crank mechanism motion with a crack in the rod can be calculated as follows:

$$\begin{aligned}
&\frac{1}{3}m_1 l_1^2\ddot{\varphi} + \frac{1}{2}m_2 l_1^2\ddot{\varphi} + \frac{1}{8}m_2\ddot{\theta}_1 l_1 l_2 = M + \frac{1}{2}m_1 g \cdot \cos\varphi \cdot l_1 + \frac{1}{2}m_2 g \cdot \cos\theta_1 \cdot l_1 + \left(\frac{1}{8}m_2 g \cdot l_2 \cdot \cos\theta_1 + T_{c01}\right) \cdot \frac{\dot{\theta}_1}{\dot{\varphi}} \\
&\frac{1}{32}m_2\ddot{\theta}_1 l_2^2 + \frac{1}{8}m_2\ddot{\varphi} l_1 l_2 + \frac{1}{24}m_2 l_2^2\ddot{\theta}_1 = T_{c01} + \frac{1}{8}m_2 g \cdot \cos\theta_1 l_2 + \left(M + m_1 g \cdot \cos\varphi \cdot \frac{1}{2}l_1\right) \cdot \frac{\dot{\varphi}}{\delta\theta_1} \\
&\frac{7}{24} \cdot m_2 \cdot l_2^2 \cdot \ddot{\theta}_2 = T_{c02} + \frac{1}{8} \cdot m_2 g \cdot \cos\theta_2 \cdot \frac{l_2}{\delta\theta_2} \\
&m_3 \cdot \ddot{s} = F \\
&\theta_c = \theta_1(x_c) - \theta_2(x_2) = \frac{C}{EI}M_1(x_c) \\
&C = 5.346h\left(1.8624\varepsilon^2 - 3.95\varepsilon^3 + 16.375\varepsilon^4 - 37.226\varepsilon^5 + 76.81\varepsilon^6 - 126.9\varepsilon^7 + 172\varepsilon^8 - 143.97\varepsilon^9 + 66.56\varepsilon^{10}\right)
\end{aligned} \tag{19}$$

Table 1: Properties of the experimental slider-crank mechanism.

| Body | Mass(kg) | Length(m) | Inertia moment(kg•m2) |
|---|---|---|---|
| Crank | 0.3 | 0.03 | 0.000072 |
| Rod | 0.036 | 0.12 | 0.0000624 |
| Slider | 1.25 | - | 0.00068 |

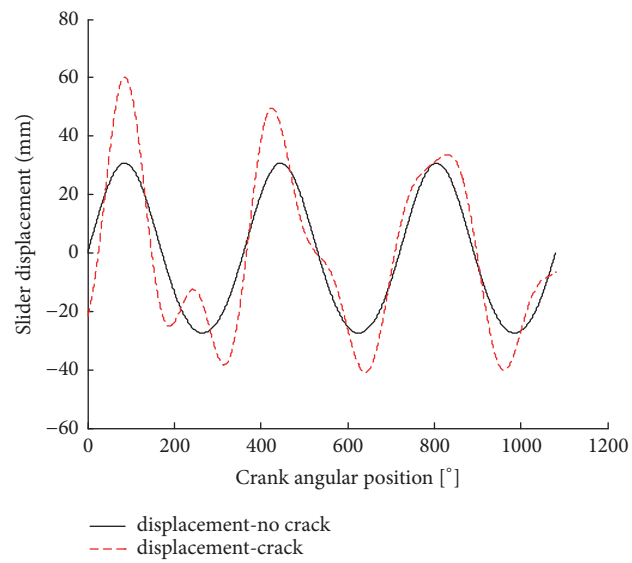


Figure 4: Displacement of slider in three cycles.

## 3. Motion Comparison of a Slider-Crank Mechanism with and without Crack in the Rod

The simulation on Slider-crank mechanism with and without crack in the rod is done based on the upper equation calculation. The mechanism is cranked by a cyclic bending moment with regular angel velocity 300RPM (revolution per minute) which means the crank is driven one cycle every 0.2s. Crack parameters used in calculation are as follows: crack depth d=6mm and cross section height h=30mm. A summary of the properties of the experimental slider-crank model is given in Table 1.

For the slider-crank mechanism with a crack in the rod, the action response of the slider is plotted versus crank angle, and the obtained results are compared with those previously obtained slider actions on the slider-crank mechanism without crack in the rod. The slider-crank mechanism without crack in the rod can be abbreviated as SC1, and the slider-crank mechanism with a crack in the rod can be abbreviated as SC2.

As shown in Figure 4, there is the comparison on slider displacement between SC1 and SC2.

(1)There is cyclic fluctuation for slider displacement on SC1, and the displacement period 360deg can be easily found in the curve. There is no clear cyclic fluctuation for slider displacement on SC2. The main reason is that SC1 is the linear system, but SC2 is the nonlinear system. Nonlinear system is much complicated and has no regular period.

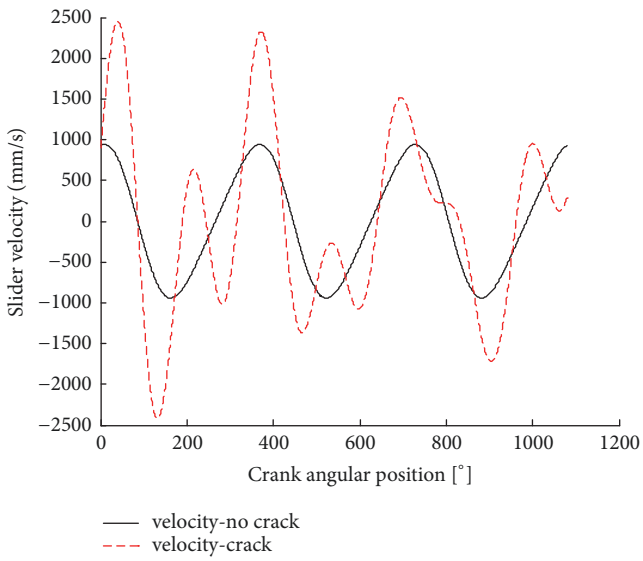


Figure 5: Velocity of slider in three cycles.

(2)The maximum for slider displacement on SC1 is lower than the maximum for slider displacement on SC2. For SC2, the slider will move on further when the slider reaches the point which is the maximum displacement for SC1, because of the different inertia influenced by the crack. Furthermore, the maximum for slider displacement on SC2 is not a definite number in each fluctuation, due to the crack lead to a complicated nonlinear vibration system.

(3)The slider displacement fluctuation tendency is the same between SC1 and SC2. That is because the crack just changes SC2 inertia and then changes the displacement. But the system motion tendency should be the same.

(4)The slider trial on SC1 is exactly symmetrical. The slider trial on SC2 is not symmetrical; for example, at the beginning fluctuation, there is one sine wave in positive direction, and there are two sine waves (one bigger sine, one smaller sine) in negative direction. The reason is the two sine waves happened during the crank pull the crack rod change to push the rod, and then the crack depth d changed.

As shown in Figure 5, there is the comparison on slider velocity between SC1 and SC2.

(1)There is cyclic fluctuation for slider velocity on SC1, and the period is 360deg which can be easily found. There is no clear cyclic fluctuation for slider velocity on SC2. The main reason is the same with displacement analysis.

(2)The maximum velocity on SC1 is much lower than the slider of SC2. The main reason is the same with displacement analysis.

As shown in Figure 6, there is the comparison on slider acceleration between SC1 and SC2.

(1)There is cyclic fluctuation for slider acceleration on SC1, and the period is 360deg which can be easily found. There is no clear cyclic fluctuation for slider acceleration on SC2. The main reason is the same with displacement analysis.

(2)The maximum of slider acceleration on SC1 is much lower than the value on SC2, which is the same with the displacement-velocity curve.

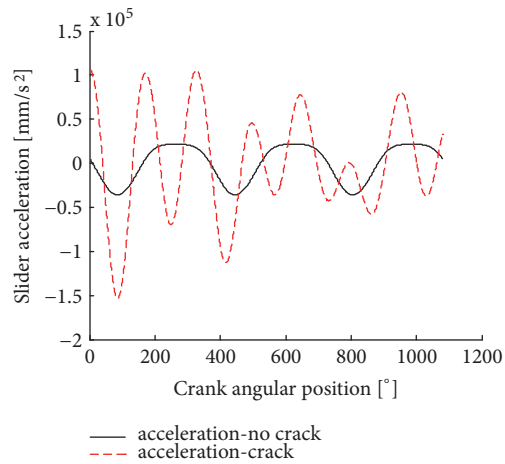


Figure 6: Acceleration of slider in three cycles.

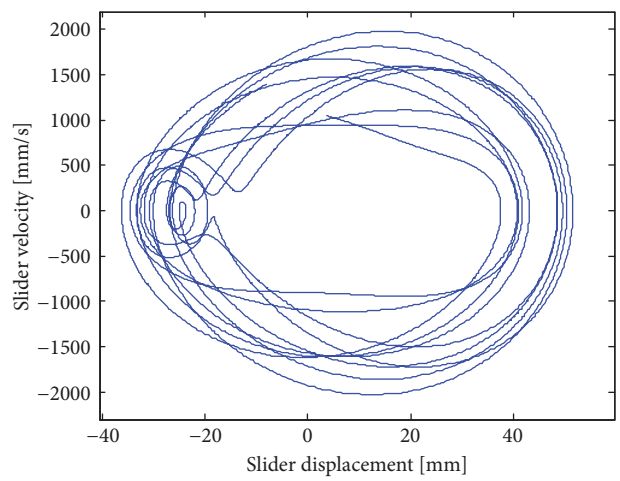


Figure 7: Phase trajectories of slider displacement-slider velocity.

From Figures 4, 5, and 6, we can see that the displacement, velocity, and acceleration of the slider are all nonperiodic signals.

## 4. Nonlinear Dynamic Analysis

Nonlinear dynamics are often characterized by a chaotic behaviour of the system. Figures 7 and 8 show that the phase trajectories of displacement-velocity and velocity-acceleration for the slider under the conditions of crank angular velocity 300 RPM.

From Figures 7 and 8, it can be seen that the phase space curve fluctuates obviously, and there will be a deviation between different periods. The motion trajectory of the nonrepetition of the ring surface in the phase diagram shows that the system is in the quasiperiodic state.

Lyapunov exponent $\lambda$ is a good method to evaluate the system sensitivity based on initial condition, and it can be used to distinguish chaotic and nonchaotic. Negative and zero Lyapunov exponent means convergence to a predictable motion, and only one positive exponent will lead to a chaotic

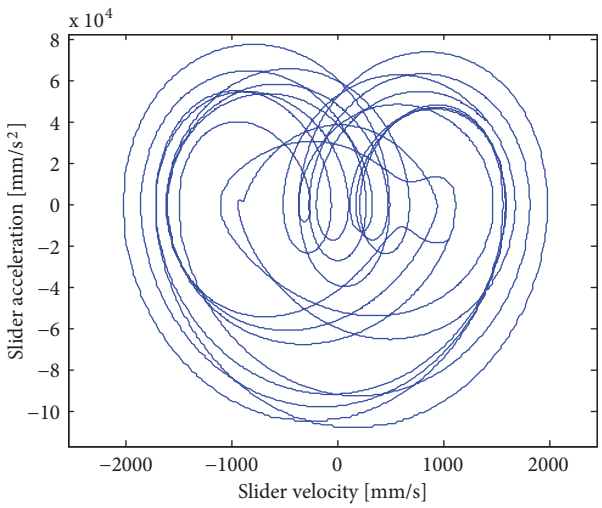


Figure 8: Phase trajectories of slider velocity-slider acceleration.

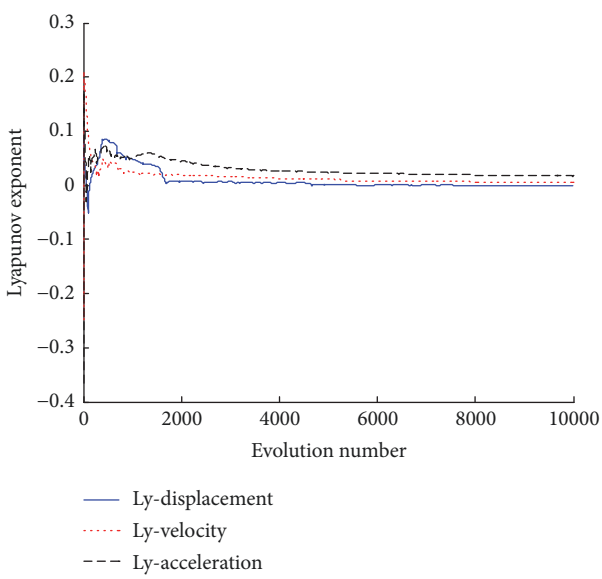


Figure 9: Lyapunov exponent of Slider on SC2.

system. To estimate the Lyapunov exponent of time series, several approaches are suggested, like the method of Wolff, Kantz, or Rosenstein [35–39].

The Lyapunov exponent is shown in Figure 9 for the system of slider-crank mechanism with a crack in the rod. The displacement, speed, and acceleration of the slider Lyapunov exponent value are 0.0095, 0.0147, and 0.0301, respectively, which means it is chaotic system. That exactly explains why there is no regular period for the slider displacement, velocity, and acceleration on SC2.

## 5. Conclusions

The motion of slider-crank mechanism with a crack in the rod is analyzed by dividing the system into two systems linked by the crack. The crack of the mechanism is simulated by using massless torsional spring. After comparing with slider displacement, velocity, and acceleration between SC1 and SC2, we can conclude that the effect of impact with crack should not be ignored when analyzing the dynamic performance. The whole curve is periodic for the slider motion on SC1, whereas it is chaotic for SC2.

## Data Availability

The data used to support the findings of this study are included within the article.

## Conflicts of Interest

The authors declare that there are no conflicts of interest regarding the publication of this paper.

## Acknowledgments

This work is supported by the Natural Science Foundation of China (51575331).

## References

[1] X. Chen and D.-W. Lee, "A microcantilever system with slider-crank actuation mechanism," *Sensors and Actuators A: Physical*, vol. 226, pp. 59–68, 2015.

[2] S. Wang, Y. Zi, Z. Wan, B. Li, and Z. He, "Effects of multiple cracks on the forced response of centrifugal impellers," *Mechanical Systems and Signal Processing*, vol. 60, pp. 326–343, 2015.

[3] U. Andreaus and P. Casini, "Identification of multiple open and fatigue cracks in beam-like structures using wavelets on deflection signals," *Continuum Mechanics and Thermodynamics*, vol. 28, no. 1-2, pp. 361–378, 2016.

[4] J. Zeng, H. Ma, W. Zhang, and B. Wen, "Dynamic characteristic analysis of cracked cantilever beams under different crack types," *Engineering Failure Analysis*, vol. 74, pp. 80–94, 2017.

[5] U. Andreaus, P. Casini, and F. Vestroni, "Frequency reduction in elastic beams due to a stable crack: numerical results compared with measured test data," *Engineering Transactions*, vol. 51, no. 1, pp. 87–101, 2003.

[6] U. Andreaus, P. Casini, and F. Vestroni, "Nonlinear features in the dynamic response of a cracked beam under harmonic forcing," in *Proceedings of the DETC2005: ASME International Design Engineering Technical Conferences and Computers and Information in Engineering Conference*, pp. 2083–2089, USA, September 2005.

[7] U. Andreaus, P. Casini, and F. Vestroni, "Non-linear dynamics of a cracked cantilever beam under harmonic excitation," *International Journal of Non-Linear Mechanics*, vol. 42, no. 3, pp. 566–575, 2007.

[8] M. Dupac and D. G. Beale, "Dynamic analysis of a flexible linkage mechanism with cracks and clearance," *Mechanism and Machine Theory*, vol. 45, no. 12, pp. 1909–1923, 2010.

[9] A. Carpinteri, A. Spagnoli, and S. Vantadori, "An elastic-plastic crack bridging model for brittle-matrix fibrous composite beams under cyclic loading," *International Journal of Solids and Structures*, vol. 43, no. 16, pp. 4917–4936, 2006.

[10] O. Giannini, P. Casini, and F. Vestroni, "Nonlinear harmonic identification of breathing cracks in beams," *Computers & Structures*, vol. 129, pp. 166–177, 2013.

[11] P. Cacciola and G. Muscolino, "Dynamic response of a rectangular beam with a known non-propagating crack of certain or uncertain depth," *Computers & Structures*, vol. 80, no. 27, pp. 2387–2396, 2002.

[12] U. Andreaus, P. Baragatti, P. Casini, and D. Iacoviello, "Experimental damage evaluation of open and fatigue cracks of multi-cracked beams by using wavelet transform of static response via image analysis," *Structural Control and Health Monitoring*, vol. 24, no. 4, 2017.

[13] M. V. Menshykova, O. V. Menshykov, and I. A. Guz, "An iterative BEM for the dynamic analysis of interface crack contact problems," *Engineering Analysis with Boundary Elements*, vol. 35, no. 5, pp. 735–749, 2011.

[14] K. Russell and R. S. Sodhi, "On the design of slider-crank mechanisms. Part II: multi-phase path and function generation," *Mechanism and Machine Theory*, vol. 40, no. 3, pp. 301–317, 2005.

[15] G. Figliolini, M. Conte, and P. Rea, "Algebraic algorithm for the kinematic analysis of slider-crank/rocker mechanisms," in *Proceedings of the ASME 2010 International Design Engineering Technical Conferences and Computers and Information in Engineering Conference, IDETC/CIE2010*, pp. 743–752, Canada, August 2010.

[16] S. S. Balli and S. Chand, "Defects in link mechanisms and solution rectification," *Mechanism and Machine Theory*, vol. 37, no. 9, pp. 851–876, 2002.

[17] K.-L. Ting, C. Xue, J. Wang, and K. R. Currie, "Mobility criteria of planar single-loop N-bar chains with prismatic joints," in *Proceedings of the ASME 2008 International Design Engineering Technical Conferences and Computers and Information in Engineering Conference, IDETC/CIE2008*, pp. 1513–1519, USA, August 2008.

[18] C. S. Koshy, P. Flores, and H. M. Lankarani, "Study of the effect of contact force model on the dynamic response of mechanical systems with dry clearance joints: computational and experimental approaches," *Nonlinear Dynamics*, vol. 73, no. 1-2, pp. 325–338, 2013.

[19] A. L. Schwab, J. P. Meijaard, and P. Meijers, "A comparison of revolute joint clearance models in the dynamic analysis of rigid and elastic mechanical systems," *Mechanism and Machine Theory*, vol. 37, no. 9, pp. 895–913, 2002.

[20] P. Flores, J. Ambrósio, and J. P. Claro, "Dynamic analysis for planar multibody mechanical systems with lubricated joints," *Multibody System Dynamics*, vol. 12, no. 1, pp. 47–74, 2004.

[21] P. Flores, J. Ambrósio, J. C. P. Claro, H. M. Lankarani, and C. S. Koshy, "Lubricated revolute joints in rigid multibody systems," *Nonlinear Dynamics*, vol. 56, no. 3, pp. 277–295, 2009.

[22] A. Bovsunovsky and C. Surace, "Non-linearities in the vibrations of elastic structures with a closing crack: a state of the art review," *Mechanical Systems and Signal Processing*, vol. 62, pp. 129–148, 2015.

[23] M. Kisa and J. Brandon, "Effects of closure of cracks on the dynamics of a cracked cantilever beam," *Journal of Sound and Vibration*, vol. 238, no. 1, pp. 1–18, 2000.

[24] W. Wang, J. Gao, L. Huang, and Z. Xin, "Experimental investigation on vibration control of rotor-bearing system with active magnetic exciter," *Chinese Journal of Mechanical Engineering*, vol. 24, no. 6, pp. 1013–1021, 2011.

[25] E. I. Shifrin and R. Ruotolo, "Natural frequencies of a beam with an arbitrary number of cracks," *Journal of Sound and Vibration*, vol. 222, no. 3, pp. 409–423, 1999.

[26] C. S. Shin and C. Q. Cai, "Fatigue crack propagation properties from small sized rod specimens," *Nuclear Engineering and Design*, vol. 236, no. 24, pp. 2574–2579, 2006.

[27] M. Skrinar and T. Plibersek, "New linear spring stiffness definition for displacement analysis of cracked beam elements," *PAMM*, vol. 4, no. 1, pp. 654-655, 2004.

[28] R. K. Behera, A. Pandey, and D. R. Parhi, "Numerical and experimental verification of a method for prognosis of inclined edge crack in cantilever beam based on synthesis of mode shapes," *Procedia Technology*, vol. 14, pp. 67–74, 2014.

[29] W. L. Bayissa and N. Haritos, "Experimental investigation into vibration characteristics of a cracked RC T-beam," Tech. Rep., Melbourne University Private Ltd, 2006.

[30] U. Andreaus and P. Baragatti, "Fatigue crack growth, free vibrations, and breathing crack detection of aluminium alloy and steel beams," *Journal of Strain Analysis for Engineering Design*, vol. 44, no. 7, pp. 595–608, 2009.

[31] U. Andreaus and P. Baragatti, "Cracked beam identification by numerically analysing the nonlinear behaviour of the harmonically forced response," *Journal of Sound and Vibration*, vol. 330, no. 4, pp. 721–742, 2011.

[32] U. Andreaus and P. Baragatti, "Experimental damage detection of cracked beams by using nonlinear characteristics of forced response," *Mechanical Systems and Signal Processing*, vol. 31, pp. 382–404, 2012.

[33] N. Pugno, C. Surace, and R. Ruotolo, "Evaluation of the nonlinear dynamic response to harmonic excitation of a beam with several breathing cracks," *Journal of Sound and Vibration*, vol. 235, no. 5, pp. 749–762, 2000.

[34] Y. Lin and F. Chu, "Stiffness models for the cracked shaft of the rotor system," *Jixie Gongcheng Xuebao/Chinese Journal of Mechanical Engineering*, vol. 44, no. 1, pp. 114–120, 2008.

[35] L. Zhenping, L. Yuegang, and Y> Hongliang, "Dynamics of rotor-bearing system with coupling faults of crack and rub-impact," *Chinese Journal of Applied Mechanics*, vol. 20, no. 3, pp. 136–141, 2003.

[36] Y. Luo, Y. Du, X. Liu, and B. Wen, "Study on dynamics and fault characteristics of two-span rotor-bearing system with pedestal looseness," *Jixie Qiangdu/Journal of Mechanical Strength*, vol. 28, no. 3, pp. 327–331, 2006.

[37] C. Liu, H. Yao, H. Li, and B. Wen, "Stability of periodic motion and experimental research on the rotor-bearing system with rub-impact and crack," *Yingyong Lixue Xuebao/Chinese Journal of Applied Mechanics*, vol. 21, no. 4, pp. 52–55, 2004.

[38] Y. Luo, P. Wang, and B. Wen, "Stability of periodic motion on the rotor-bearing system with crack and rub-impact," *Journal of Mechanical Science and Technology*, vol. 25, no. Issue 6, pp. 705–707, 2006.

[39] Q. Tian, Y. Zhang, L. Chen, and P. Flores, "Dynamics of spatial flexible multibody systems with clearance and lubricated spherical joints," *Computers & Structures*, vol. 87, no. 13-14, pp. 913–929, 2009.